

## Quasiparticle Lifetime in Ultracold Fermionic Mixtures with Density and Mass Imbalance

Zhihao Lan,<sup>1,\*</sup> Georg M. Bruun,<sup>2</sup> and Carlos Lobo<sup>1</sup>

<sup>1</sup>*Mathematical Sciences, University of Southampton, Highfield, Southampton, SO17 1BJ, United Kingdom*

<sup>2</sup>*Department of Physics and Astronomy, University of Aarhus, Ny Munkegade, DK-8000 Aarhus C, Denmark*  
(Received 1 February 2013; revised manuscript received 15 May 2013; published 2 October 2013)

We show that atomic Fermi mixtures with density and mass imbalance exhibit a rich diversity of scaling laws for the quasiparticle decay rate beyond the quadratic energy and temperature dependence of conventional Fermi liquids. For certain densities and mass ratios, the decay rate is linear, whereas in other cases, it exhibits a plateau. Remarkably, this plateau extends from the deeply degenerate to the high temperature classical regime of the light species. Many of these scaling laws are analogous to what is found in very different systems, including dirty metals, liquid metals, and high temperature plasmas. The Fermi mixtures can in this sense span a whole range of seemingly diverse and separate physical systems. Our results are derived in the weakly interacting limit, making them quantitatively reliable. The different regimes can be detected with radio-frequency spectroscopy.

DOI: [10.1103/PhysRevLett.111.145301](https://doi.org/10.1103/PhysRevLett.111.145301)

PACS numbers: 67.85.Lm, 34.50.-s, 71.10.Ay

*Introduction.*—There are many systems in nature composed of two different types of fermions with either different concentrations or different masses, such as electron-ion plasmas, liquid metals, spin-polarized conductors, and certain cases of nuclear matter. The temperature in these systems usually lies in a characteristic range with respect to the Fermi temperatures of the two components. For example, in spin-polarized conductors, both spin states are fully degenerate, while in hot electron-ion plasmas, both are fully classical. An interesting class of systems appears when one of the components is degenerate while the other is classical. This occurs, for example, in spin-polarized Fermi gases when the minority component is classical [1,2], liquid metals, and in warm dense matter, a type of plasma where the ions are classical but the electrons are close to degeneracy [3]. We show in this Letter that two-component Fermi mixtures of ultracold atoms provide the possibility for the first time to access all of these disparate regimes within a single experimental system. For example, mixtures of <sup>6</sup>Li and <sup>40</sup>K have already been created [2] where the <sup>6</sup>Li atoms are degenerate but where the <sup>40</sup>K atoms can be either above or below their Fermi temperature. In these mixtures, we demonstrate that various regimes of temperature and concentration difference give rise to a variety of energy and temperature scalings of the lifetime of the majority quasiparticles that are analogous to several of the very different Fermi mixtures in nature. Contrary to plasmas or the electron gas, which in general are extremely complex to describe, ultracold atomic gases interact via a short range interaction which is accurately characterized by the scattering length, and the effects discussed in this Letter are all realized in the weak coupling regime. This means that the quasiparticle lifetime is described by a compact and reliable expression involving the Lindhard function, which nevertheless contains all the different physics in various limits and the interpolations between them.

The reason for the appearance of these scaling laws is that in a system with two types of atom (which we will denote by “↑” and “↓”) of different masses and/or densities, the Fermi energies of the two species are in general unequal, leading to the existence of two energy (and temperature) scales. We will assume here that  $\varepsilon_{F\downarrow} \ll \varepsilon_{F\uparrow}$ . The difference can be due to a large density imbalance  $n_{\downarrow} \ll n_{\uparrow}$  with equal mass or large mass imbalance  $m_{\downarrow} \gg m_{\uparrow}$  with equal density. This results in an intermediate-energy regime  $\varepsilon_{F\downarrow} \ll \varepsilon \ll \varepsilon_{F\uparrow}$  which increases in size with mass or density imbalance. While the quadratic behavior of Fermi liquids is due to the effect of Pauli blocking of both species [4], the key property of this intermediate regime is that the Pauli blocking of the ↓ atoms is unimportant, so that the phase space for interspecies scattering depends only on the ↑ atoms. We will show that for the  $n_{\downarrow} \ll n_{\uparrow}$  equal mass mixture, the Pauli blocking of ↑ atoms results in a linear decay rate in temperature, while for a  $m_{\downarrow} \gg m_{\uparrow}$  equal density mixture, energy conservation restricts the phase space for scattering of the ↑ atoms to a narrow region around the Fermi surface, making Pauli blocking of the ↑ atoms irrelevant, leading to a temperature-independent decay rate. The effects on the lifetime due to the modification of Pauli blocking in spin-polarized Fermi systems were known in spin-polarized liquid <sup>3</sup>He and ferromagnetic metals [5–7]. For example, they are responsible for the observed zero temperature damping of the transverse spin dynamics in spin-polarized <sup>3</sup>He [5,6]. Experimentally, Fermi mixtures with density imbalance [8,9] or mass imbalance [10–12] have been created, which raises the prospect of observing the effects we discuss here in the near future using, for instance, radio-frequency (rf) spectroscopy.

*Model.*—We consider a homogeneous gas of two species of fermions denoted  $\sigma = \uparrow, \downarrow$  with masses  $m_{\downarrow} \leq m_{\uparrow}$  and densities  $n_{\downarrow} \geq n_{\uparrow}$ , from which we define the Fermi

momenta  $k_{F\sigma} \equiv (6\pi^2 n_\sigma)^{1/3}$ . The key quantity we study in this Letter is the decay rate  $1/\tau_p$  of the  $\uparrow$  quasiparticles with momentum  $\mathbf{p}$  and energy  $\varepsilon_{p\uparrow}$ . To lowest order in the scattering processes, the decay rate can be written as [13]

$$\frac{1}{\tau_p} = 2\pi U^2 \sum_{\mathbf{k}} \sum_{\mathbf{q}} \delta(\varepsilon_{p\uparrow} + \varepsilon_{\mathbf{k}\downarrow} - \varepsilon_{\mathbf{p}-\mathbf{q}\downarrow} - \varepsilon_{\mathbf{k}+\mathbf{q}\downarrow}) \times [n_{\mathbf{k}\downarrow}(1 - n_{\mathbf{k}+\mathbf{q}\downarrow})(1 - n_{\mathbf{p}-\mathbf{q}\downarrow}) + (1 - n_{\mathbf{k}\downarrow})n_{\mathbf{k}+\mathbf{q}\downarrow}n_{\mathbf{p}-\mathbf{q}\downarrow}], \quad (1)$$

where  $n_{\mathbf{k}\sigma} = (e^{\beta\varepsilon_{\mathbf{k}\sigma}} + 1)^{-1}$  is the Fermi function. We have defined  $\xi_{\mathbf{p}\sigma} = \varepsilon_{\mathbf{p}\sigma} - \mu_\sigma$ , with  $\mu_\sigma$  the chemical potential, and  $\beta = 1/T$ , with  $T$  the temperature (we set  $k_B = \hbar = 1$ ). The energy is  $\varepsilon_{p\sigma} = p^2/2m_\sigma$ , where  $m_\sigma$  is the effective mass. The parameter  $U$  is the effective interaction between the  $\uparrow$  and the  $\downarrow$  atoms, and we have neglected interactions between identical atoms for simplicity. In the strong coupling regime, one can extract the value of the effective mass and  $U$  from Monte Carlo, variational, and thermodynamic arguments [14–16]. We will mostly work in the weak coupling regime, where we have  $U = 2\pi a/m_r$  and where  $m_r = m_\uparrow m_\downarrow / (m_\uparrow + m_\downarrow)$  is the reduced mass and  $a$  the scattering length for the interaction between the two atom species [17].

For analytic investigation, it is convenient to rewrite Eq. (1) in terms of the imaginary part of the Lindhard function of the  $\downarrow$  atoms given by [18]

$$\text{Im}\chi_1(q, \omega) = -\pi \int \frac{d^3k}{(2\pi)^3} (n_{\mathbf{k}\downarrow} - n_{\mathbf{k}+\mathbf{q}\downarrow}) \delta(\omega - \varepsilon_{\mathbf{k}+\mathbf{q}\downarrow} + \varepsilon_{\mathbf{k}\downarrow}). \quad (2)$$

To do this, we first recast the  $\delta$  function in Eq. (1) in the form  $\delta(\varepsilon_{p\uparrow} + \varepsilon_{\mathbf{k}\downarrow} - \varepsilon_{\mathbf{p}-\mathbf{q}\downarrow} - \varepsilon_{\mathbf{k}+\mathbf{q}\downarrow}) = \int_{-\infty}^{+\infty} d\omega \delta(\omega - \varepsilon_{p\uparrow} + \varepsilon_{\mathbf{p}-\mathbf{q}\downarrow}) \delta(\omega - \varepsilon_{\mathbf{k}+\mathbf{q}\downarrow} + \varepsilon_{\mathbf{k}\downarrow})$ . We also use the Fermi function identities  $n_{\mathbf{k}\downarrow}(1 - n_{\mathbf{k}+\mathbf{q}\downarrow}) = (n_{\mathbf{k}\downarrow} - n_{\mathbf{k}+\mathbf{q}\downarrow}) / (1 - e^{-\beta\omega})$  and  $(1 - n_{\mathbf{k}\downarrow})n_{\mathbf{k}+\mathbf{q}\downarrow} = (n_{\mathbf{k}\downarrow} - n_{\mathbf{k}+\mathbf{q}\downarrow}) / (e^{\beta\omega} - 1)$ , with  $\omega \equiv \varepsilon_{\mathbf{k}+\mathbf{q}\downarrow} - \varepsilon_{\mathbf{k}\downarrow}$ . Finally, the angular integral over  $\mathbf{q}$  is  $\int \Omega_q \delta(\omega - \varepsilon_{p\uparrow} + \varepsilon_{\mathbf{p}-\mathbf{q}\downarrow}) = 2\pi m_\uparrow / pq$  with  $-pq/m_\uparrow - q^2/2m_\uparrow \leq \omega \leq pq/m_\uparrow - q^2/2m_\uparrow$ , and we obtain

$$\frac{1}{\tau_p} = -\frac{m_\uparrow |U|^2}{2\pi^2 p} \int_0^\infty dq q \int_{\omega_-}^{\omega_+} d\omega \text{Im}\chi_1(q, \omega) F(\omega, \varepsilon_{p\uparrow}, \mu_\uparrow), \quad (3)$$

where  $F(\omega, \varepsilon_{p\uparrow}, \mu_\uparrow) = (1 + e^{\beta(\omega - \xi_{p\uparrow})})^{-1} (1 - e^{-\beta\omega})^{-1} + (1 + e^{-\beta(\omega - \xi_{p\uparrow})})^{-1} (e^{\beta\omega} - 1)^{-1}$  and  $\omega_\pm(q) = \pm pq/m_\uparrow - q^2/2m_\uparrow$ .

Before proceeding, let us briefly discuss the difference between the situation considered here and the usual quadratic Fermi liquid behavior. In a conventional Fermi liquid, the low-energy condition  $\xi_p = \varepsilon_p - \mu \ll \varepsilon_F$  and  $T \ll \varepsilon_F$  ensures that one can use  $\text{Im}\chi_1(q, \omega) \propto \omega/q$  in Eq. (3), leading to quadratic scaling of the decay rate

with energy and temperature. Here, the Lindhard function of the  $\downarrow$  atoms has a different behavior in the intermediate regime, which will result in different power laws.

*Zero temperature.*—In the following, we will take  $\xi_{p\uparrow} \geq 0$  without loss of generality since  $\tau_p(\xi)$  is an even function for  $|\xi| \ll \varepsilon_{F\uparrow}$ . In this case, the backscattering term [the second term in Eq. (3)] vanishes at  $T = 0$ . The integration region in Eq. (3) is determined by three conditions: from the Bose factors, we have  $0 \leq \omega \leq \xi_{p\uparrow}$ ;  $\omega \leq \omega_+(q)$  and  $0 \leq q \leq 2p$ . Using the  $T = 0$  expression for the Lindhard function [18]  $\text{Im}\chi_1(q, \omega) = -m_\downarrow^2 \varepsilon_{F\downarrow} / 4\pi q [\Theta(1 - v_-^2)(1 - v_-^2) - \Theta(1 - v_+^2)(1 - v_+^2)]$  with  $v_\pm = m_\downarrow \omega / q k_{F\downarrow} \pm q / 2k_{F\downarrow}$ , we obtain

$$\frac{1}{\tau_p} = \frac{|U|^2 m_\uparrow m_\downarrow^2 \varepsilon_{F\downarrow}}{8\pi^3 p} \int_0^{2p} dq \int_0^{\xi_{p\uparrow}, \omega_+} d\omega [\Theta(1 - v_-^2)(1 - v_-^2) - \Theta(1 - v_+^2)(1 - v_+^2)]. \quad (4)$$

(i) The low-energy regime  $\xi_{p\uparrow} \ll \varepsilon_{F\downarrow} \ll \varepsilon_{F\uparrow}$ . When the energy is small compared to both Fermi energies, we can use  $\text{Im}\chi_1(q, \omega) = -m_\downarrow^2 \omega / 4\pi q$ , which gives

$$\frac{1}{\tau_p} = \frac{|U|^2 m_\uparrow m_\downarrow^2 k_{F\downarrow}}{8\pi^3 p} \xi_{p\uparrow}^2. \quad (5)$$

This is the usual quadratic dependence of the decay rate on excitation energy characteristic of a conventional Fermi liquid. Indeed, when  $m_\downarrow = m_\uparrow$ , we recover the well-known expression for the damping rate of a quasiparticle at  $T = 0$  [18].

(ii) The intermediate regime  $\varepsilon_{F\downarrow} < \xi_{p\uparrow} < \gamma \varepsilon_{F\downarrow} \ll \varepsilon_{F\uparrow}$  with  $\gamma = 4(k_{F\uparrow}/k_{F\downarrow} - 1)(k_{F\uparrow}/k_{F\downarrow} + m_\uparrow/m_\downarrow) / (1 + m_\uparrow/m_\downarrow)^2$ , where  $\gamma \varepsilon_{F\downarrow}$  is defined as the  $\omega$  coordinate of the intersection of the  $\omega_+$  and  $v_- = -1$  curves (for this region to exist, apart from the main effect of mass imbalance, we must have  $\gamma > 1$ , which also sets a condition on the density imbalance). We obtain

$$\frac{1}{\tau_p} = \frac{|U|^2 m_\uparrow m_\downarrow^2 n_{F\downarrow}}{2\pi p} \left( \xi_{p\uparrow} - \frac{2}{5} \varepsilon_{F\downarrow} \right). \quad (6)$$

The linear dependence of the decay rate is also characteristic of marginal Fermi liquids [19], although the physics there is quite different and the linear scaling is due to strong spin fluctuations. In Fig. 1, we plot the decay at zero temperature as a function of the excitation energy. We have chosen the parameters  $m_\downarrow/m_\uparrow = 173/6$ , corresponding to a mixture of  $^{173}\text{Yb}$  and  $^6\text{Li}$  atoms [10], and  $k_{F\uparrow}/k_{F\downarrow} = 2$ . These parameters give  $\varepsilon_{F\uparrow}/\varepsilon_{F\downarrow} = 115$ , corresponding to a large regime of intermediate energies. Both the usual quadratic and linear scalings are clearly visible in Fig. 1.

*Nonzero temperature, degenerate case.*—In this regime, we have  $0 < T \ll T_{F\uparrow}$  and we consider the case  $\xi_{p\uparrow} = 0$ . From the thermal distribution functions in Eq. (3), it follows that the integrand is significant only in the range  $|\omega| \lesssim T$ . Since  $T \ll T_{F\uparrow}$ , we can approximate Eq. (3) by

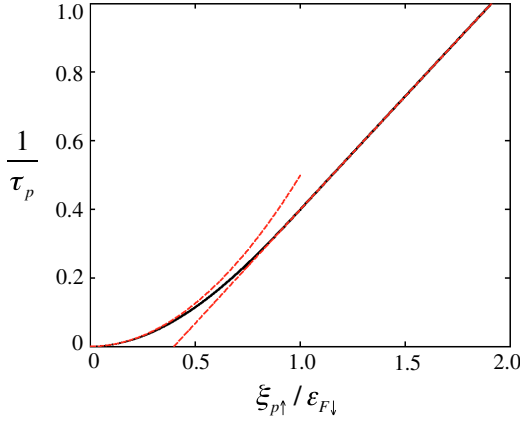


FIG. 1 (color online). Zero temperature decay rate  $1/\tau_p$  (units of  $|U|^2 m_1^2 \epsilon_{F1}^2 / 8\pi^3$ ) of an  $\uparrow$  quasiparticle as a function of excitation energy  $\xi_{p1}$ , with  $m_1/m_1 = 173/6$  and  $k_{F1}/k_{F1} = 2$ . The solid black curve is the result of a numerical integration of Eq. (3), and the dashed red curves are given by Eqs. (5) and (6).

$$\frac{1}{\tau_{k_{F1}}} = -\frac{|U|^2 m_1}{2\pi^2 k_{F1}} \int_0^{2k_{F1}} q dq \int_{-\infty}^{\infty} \frac{2\text{Im}\chi_1(q, \omega) d\omega}{(e^{\beta\omega} + 1)(1 - e^{-\beta\omega})}. \quad (7)$$

(i)  $T \ll T_{F1}$ . In this case, we can use the zero temperature, low-energy expression  $\text{Im}\chi_1(q, \omega) = -m_1^2 \omega / 4\pi q$  to obtain

$$\frac{1}{\tau_{k_{F1}}} = \frac{|U|^2 m_1^2 k_{F1}}{8\pi k_{F1}} T^2. \quad (8)$$

Here, the system has the quadratic Fermi liquid behavior and we recover the standard result when  $T_{F1} = T_{F1}$  [18].

(ii)  $T_{F1} \ll T \ll T_{F1}$ . The gas of  $\downarrow$  atoms is now classical, and we can use the expression  $\text{Im}\chi_1(q, \omega, T) = -\pi n_1 \sqrt{2m_1 \beta / \pi} e^{-\omega^2 m_1 \beta / 2q^2} e^{-q^2 \beta / 8m_1} \sinh(\beta\omega/2) / q$  [16]. The decay rate can then be written as

$$\frac{1}{\tau_{k_{F1}}} = \frac{2|U|^2 m_1 m_1 n_1 T}{\pi^{3/2} k_{F1}} I\left(\sqrt{k_{F1}^2 / 2m_1 T}\right) \quad (9)$$

with

$$I(t) \equiv \int_0^t dy e^{-y^2} \int_{-\infty}^{\infty} dx \frac{e^{-x^2/4y^2}}{\cosh x}. \quad (10)$$

We now discuss two important special cases of Eqs. (9) and (10). First, we consider the case of a highly polarized system of two spin states of the same atom, i.e.,  $m_1 = m_1 = m$  and  $n_1 \ll n_1$ . In this case, we have  $\sqrt{k_{F1}^2 / 2mT} = \sqrt{T_{F1}/T} \gg 1$ . Using  $I(\infty) = \sqrt{\pi} \ln 2$ , we obtain

$$\frac{1}{\tau_{k_{F1}}} = 2 \ln 2 \frac{|U|^2 m^2 n_1}{\pi k_{F1}} T. \quad (11)$$

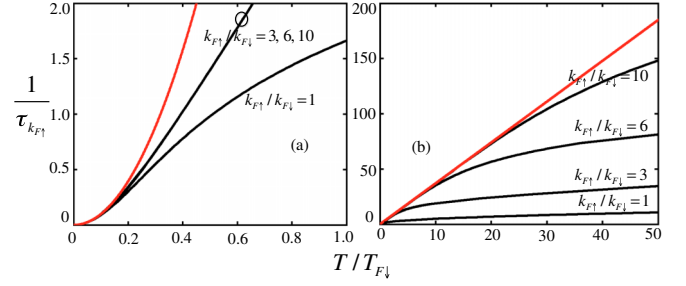


FIG. 2 (color online). Decay rate  $1/\tau_{k_{F1}}$  in units of  $|U|^2 m^3 \epsilon_{F1}^2 k_{F1} / 8\pi^3 k_{F1}$  as a function of temperature with  $m_1 = m_1 = m$  for different density imbalances  $k_{F1}/k_{F1} = 1, 3, 6, 10$ . The solid black (dark) curves are the numerical integration of Eq. (3), while the solid red (light) curves in (a) and (b) are given by Eqs. (8) and (11), respectively.

In Fig. 2, we plot the decay rate  $1/\tau_{k_{F1}}$  as a function of  $T$  for several density imbalances. In Fig. 2(a), we see the quadratic low temperature behavior. Note that the curves for  $k_{F1}/k_{F1} = 3, 6, 10$  overlap in this range. In Fig. 2(b), we see the appearance of linear scaling. The range of linear temperature scaling increases with the density imbalance.

The second case we consider is that of an equal density mixture of heavy and light atoms ( $m_1 \ll m_1$  and  $n_1 \equiv n_1 = n_1$ ), so that  $\sqrt{k_{F1}^2 / 2m_1 T} = \sqrt{T_{F1}/T} \ll 1$ . Since  $I(t) \approx \sqrt{\pi} t^2 (1 - t^2)$  for  $t \ll 1$ , we find that

$$\frac{1}{\tau_{k_{F1}}} = \frac{|U|^2 m_1 n_1 k_{F1}}{\pi} \left(1 - \frac{T_{F1}}{T}\right), \quad (12)$$

which shows that the decay rate is constant to leading order in  $T_{F1}/T$ . This peculiar behavior can be understood as follows. Since  $T \ll T_{F1}$ , we have  $v_{\text{thl}} \ll v_{F1}$  with  $v_{\text{thl}} = \sqrt{2T/m_1}$  and  $v_{F1} = k_{F1}/m_1$ , and the  $\downarrow$  atoms are moving very slowly compared with the  $\uparrow$  atoms. The decay rate is then dominated by the motion of the  $\uparrow$  quasiparticle:  $\tau^{-1} = n_1 \sigma_{\text{sc}} v_{F1}$ , where  $\sigma_{\text{sc}}$  is the scattering cross section. Using  $\sigma_{\text{sc}} = |U|^2 m_1^2 / \pi$  for  $m_1 \gg m_1$  [16], we get  $\tau^{-1} \sim |U|^2 m_1 n_1 k_{F1} / \pi$ , which is precisely the leading constant term of the above expression. This constant term in Eq. (12) is well known in the theory of doped semiconductors or dirty metals since there the heavy atoms correspond to the static impurities [20]. In Fig. 3, we plot the decay rate of an  $\uparrow$  excitation with momentum  $k_{F1}$  as a function of temperature. The emergence with increasing mass ratio  $m_1/m_1$  of a plateau where the rate is independent of temperature is clearly visible in Fig. 3(a). Note that this plateau extends to temperatures well above  $T_{F1}$  for large mass ratios even though the simple kinetic argument breaks down above  $T_{F1}$  since we then have to take into account the changes to the  $\uparrow$  Fermi surface which also affect the scattering rate. Instead, as we show below, the reason the plateau continues to higher temperatures is

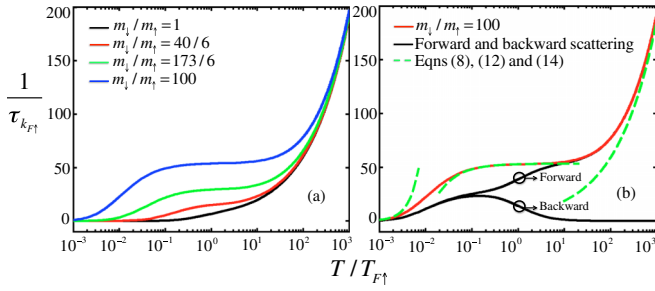


FIG. 3 (color online). Decay rate  $1/\tau_{k_{F\uparrow}}$  in units of  $|U|^2 k_F^4 m_r^2 / 32\pi^3 (m_l m_\uparrow)^{1/2}$  as a function of temperature for  $n_\uparrow = n_\downarrow$  obtained from a numerical integration of Eq. (3). The left figure shows the appearance of a plateau for  $m_l \gg m_\uparrow$ . The right figure compares the numerical results (solid curves) with Eqs. (8), (12), and (14) (dashed curves) in the low, intermediate, and high temperature limits, respectively. It also shows the contributions of the forward and backward scattering terms of Eq. (1).

because of a cancellation between the changes to the forward and backward scattering terms.

*Nonzero temperature, classical case ( $p = k_{F\uparrow}$ ).*—In the regime  $T_{F\uparrow} \ll T$ , both  $\sigma = \uparrow, \downarrow$  distributions are classical.

(i)  $T_{F\uparrow} \ll T \ll T_{F\uparrow} m_l / m_\uparrow$ . Assuming that  $U$  continues to be weakly dependent on energy and momentum (as occurs, for example, when  $k_{F\uparrow} |a| \ll 1$ ), the plateau will persist to a much larger temperature scale, given by  $v_{\text{th}\downarrow} \sim v_{F\uparrow}$  (i.e.,  $T \sim T_{F\uparrow} m_l / m_\uparrow$ ), as can be seen from the numerics (see Fig. 3). This seems to indicate that the Pauli blocking of the  $\uparrow$  atoms plays no role for the decay rate of an  $\uparrow$  quasiparticle since the plateau survives independently of whether the  $\uparrow$  atoms are degenerate ( $T \ll T_{F\uparrow}$ ) or classical ( $T \gg T_{F\uparrow}$ ). To better understand this unusual behavior, we plot in Fig. 3(b) the forward and backward scattering contributions to  $1/\tau_{k_{F\uparrow}}$  with  $m_l/m_\uparrow = 100$  [12]. We find that, when  $T \ll T_{F\uparrow}$ , the forward and backward scatterings contribute equally to  $1/\tau_{k_{F\uparrow}}$ , which can be understood by taking  $\xi_{p\uparrow} = 0$  in Eq. (3). In the regime  $T_{F\uparrow} \lesssim T \ll T_{F\uparrow} (m_l/m_\uparrow)$ , the backward scattering begins to decrease while the forward scattering increases, keeping, however, their sum constant. This shows that Pauli blocking indeed affects the forward and backward scatterings but not the sum of the two. This constant sum is due to the vanishing energy transfer in the decay process of the  $\uparrow$  quasiparticle with a large mass imbalance [ $\omega_{\text{max}}/T \sim \max(m_l/m_\downarrow, \sqrt{T_{F\downarrow}}/T) \ll 1$ ]. Thus, by rewriting  $n_{k\downarrow}(1 - n_{k+\mathbf{q}\downarrow})(1 - n_{\mathbf{p}-\mathbf{q}\uparrow}) + (1 - n_{k\downarrow})n_{k+\mathbf{q}\downarrow} = (n_{k\downarrow} - n_{k+\mathbf{q}\downarrow})/(e^{\beta\omega} - 1) [e^{\beta\omega}(1 - n_{\mathbf{p}-\mathbf{q}\uparrow}) + n_{\mathbf{p}-\mathbf{q}\uparrow}] \approx (n_{k\downarrow} - n_{k+\mathbf{q}\downarrow})/(e^{\beta\omega} - 1)$ , we see that the  $\uparrow$  atoms play no role in the integrand of Eq. (3), explaining why the plateau survives independently of whether the  $\uparrow$  atoms are degenerate or classical; i.e., the Pauli blocking is irrelevant in this case. This regime occurs also in warm dense plasmas where the electrons are close to degeneracy but the ions are already classical [3]. Note,

however, that the lifetime is likely to behave very differently since the electron-ion cross section is momentum dependent, unlike the low-energy contact interaction.

(ii)  $T_{F\uparrow} m_l / m_\uparrow \ll T$ . Using the classical limit of the chemical potential for fixed particle number in Eq. (3), i.e.,  $\mu/T \rightarrow -\infty$  when  $T \rightarrow \infty$ , we find  $1/\tau_{k_{F\uparrow}}$  is again given by Eq. (9), but with

$$I(t) = \int_0^\infty dy e^{-y^2} \int_{(-y^2-y)t(2m_l/m_\uparrow)}^{(-y^2+y)t(2m_l/m_\uparrow)} dx e^{-x^2/4y^2} e^x, \quad (13)$$

where  $t = \sqrt{k_{F\uparrow}^2 / 2m_\uparrow T}$ . When  $t \ll 1$ , the integral can be evaluated straightforwardly, which gives  $I(t) = 2tm_r^2/m_\uparrow m_l$ , and the decay rate becomes

$$\frac{1}{\tau_{k_{F\uparrow}}} = \frac{2\sqrt{2}|U|^2 m_r^2 n_\downarrow}{\pi^{3/2} \sqrt{m_\downarrow}} \sqrt{T}. \quad (14)$$

It is interesting to compare Eq. (14) with Eq. (12). First, we note that the Fermi momentum  $k_{F\uparrow}$  in Eq. (12) has been replaced by  $\sqrt{T}$  in Eq. (14), as expected for the high temperature regime. Second, when the two expressions are equated, we obtain that the crossover between the intermediate  $T$  behavior given by Eq. (12) and the high  $T$  behavior given by Eq. (14) occurs for  $T \sim T_{F\uparrow} m_l / m_\uparrow$  in agreement with the analysis above. Thus, the region where the damping rate is independent of temperature when  $n_\uparrow = n_\downarrow$  and  $m_l \gg m_\uparrow$  extends to temperatures much higher than  $T_{F\uparrow}$ . This effect is clearly illustrated in Fig. 3. Importantly, it makes the experimental observation of this plateau regime significantly easier, as it emerges already for fairly high temperatures, when the mass imbalance is large.

*Polaron case.*—Given its experimental importance, we finally calculate the collision rate of the minority particles. When  $n_\downarrow \rightarrow 0$ , i.e., in the polaron limit, we find from Eq. (1)

$$\frac{1}{\tau_\downarrow} = \frac{4}{15\pi^3} |U|^2 m_\downarrow m_\uparrow^2 \left( \varepsilon_\downarrow^2 + \frac{5\pi^2 T^2}{32} \right) \quad (15)$$

for  $\varepsilon_\downarrow \ll \varepsilon_{F\uparrow}$  and  $T \ll T_{F\uparrow}$ . The polaron therefore shows normal Fermi liquid behavior, consistent with the literature [15].

*Experimental probes.*—rf spectroscopy is a very successful method to probe the single particle properties in cold atom gases, and it is well suited to detect these new scaling laws. First, we note that the intermediate temperature regime  $T_{F\downarrow} \ll T \ll T_{F\uparrow}$  has already been achieved by the Innsbruck group using a mixture of  $^6\text{Li}$  and  $^{40}\text{K}$  atoms [2]. They probed the single particle properties of the  $\downarrow$  atoms ( $^{40}\text{K}$ ) using rf spectroscopy, where the  $^{40}\text{K}$  atoms performed Rabi oscillations between an interacting and a noninteracting state. Quasiparticle collisions cause decoherence, and the observed damping of the Rabi oscillations can therefore be used to measure the collision rate. A similar experiment should be able to detect the  $\uparrow$  collision

rate, as described by Eq. (1). One could block out the low lying states in the Fermi sea of  $\uparrow$  atoms from participating in the rf spectroscopy by coupling them to a noninteracting state with a filled Fermi sea slightly smaller than that of the  $\uparrow$  atoms. The low lying states are then inert to the rf probe due to the blocking of the noninteracting state. Alternatively, one could use momentum-resolved rf spectroscopies [2,21,22]. For a  ${}^6\text{Li}$ - ${}^{40}\text{K}$  mixture, the typical experimental parameters used in Ref. [2] are  $\varepsilon_F^{\text{Li}} = 232\hbar$  kHz and  $k_F^{\text{Li}} = \hbar^{-1}\sqrt{2m_{\text{Li}}\varepsilon_F^{\text{Li}}} = 1/2850a_0$  with  $a_0$  as Bohr's radius and the interspecies background scattering length  $a_{\text{bg}} = 63a_0$ . Assuming equal density  $n_{\text{Li}} = n_{\text{K}}$  and  $k_F a = 0.1$ , we find that the quasiparticle lifetime of Li in the plateau regime is  $\sim 1$  ms, which is the typical scale measured in Ref. [2]. In solid state systems, deviations from standard quadratic behavior often show up in electrical resistivity, specific heat, and magnetic susceptibility measurements. In atomic gases, our results could affect transport properties such as the spin drag rate (which has already been measured [23]), the damping of collective modes, and thermodynamic properties such as the heat capacity.

*Discussion and conclusions.*—We have shown that weakly interacting Fermi-Fermi mixtures realize a rich diversity of regimes for the quasiparticle damping which are analogous to several quite distinct physical systems in nature. These regimes are characterized by scaling laws for the quasiparticle lifetime which are different from the usual quadratic case. Our results are derived in the weakly interacting limit, making them quantitatively reliable. The effects described in this Letter can be measured using rf spectroscopy.

We would like to thank M. Baranov, P. Massignan, and T. Killian for discussions. Z.L. and C.L. acknowledge support from the EPSRC through Grant No. EP/I018514/1.

---

\*z.ian@soton.ac.uk

- [1] A. Schirotzek, C.-H. Wu, A. Sommer, and M. W. Zwierlein, *Phys. Rev. Lett.* **102**, 230402 (2009).
- [2] C. Kohstall, M. Zaccanti, M. Jag, A. Trenkwalder, P. Massignan, G.M. Bruun, F. Schreck, and R. Grimm, *Nature (London)* **485**, 615 (2012).
- [3] M. S. Murillo, *Phys. Plasmas* **11**, 2964 (2004).
- [4] L. D. Landau, *Sov. Phys. JETP* **3**, 920 (1957).
- [5] A. E. Meyerovich and K. A. Musaelian, *J. Low Temp. Phys.* **94**, 249 (1994).
- [6] V. P. Mineev, *Phys. Rev. B* **69**, 144429 (2004); *Phys. Rev. B* **72**, 144418 (2005).
- [7] J. Sánchez-Barriga, J. Braun, J. Minár, I. Di Marco, A. Varykhalov, O. Rader, V. Boni, V. Bellini, F. Manghi, H. Ebert, M. I. Katsnelson, A. I. Lichtenstein, O. Eriksson, W. Eberhardt, H. A. Dürr, and J. Fink, *Phys. Rev. B* **85**, 205109 (2012).
- [8] S. Nascimbène, N. Navon, K. J. Jiang, F. Chevy, and C. Salomon, *Nature (London)* **463**, 1057 (2010).
- [9] Y. Shin, C. H. Schunck, A. Schirotzek, and W. Ketterle, *Nature (London)* **451**, 689 (2008); G. B. Partridge, W. Li, R. I. Kamar, Y. Liao, and R. G. Hulet, *Science* **311**, 503 (2006).
- [10] H. Hara, Y. Takasu, Y. Yamaoka, J. M. Doyle, and Y. Takahashi, *Phys. Rev. Lett.* **106**, 205304 (2011); A. H. Hansen, A. Y. Khramov, W. H. Dowd, A. O. Jamison, B. P.-Swing, R. J. Roy, and S. Gupta, *Phys. Rev. A* **87**, 013615 (2013).
- [11] E. Wille, F. M. Spiegelhalder, G. Kerner, D. Naik, A. Trenkwalder, G. Hendl, F. Schreck, R. Grimm, T. G. Tiecke, J. T. M. Walraven, S. J. J. M. F. Kokkelmans, E. Tiesinga, and P. S. Julienne, *Phys. Rev. Lett.* **100**, 053201 (2008); L. Costa, J. Brachmann, A.-C. Voigt, C. Hahn, M. Taglieber, T. W. Hänsch, and K. Dieckmann, *Phys. Rev. Lett.* **105**, 123201 (2010).
- [12] Even for equal mass mixtures, an unequal mass mixture can be created by, e.g., imposing a spin-dependent optical lattice which can change the effective mass of one of the species by extremely large values.
- [13] G. Baym and C. J. Pethick, *Landau Fermi-Liquid Theory* (Wiley-VCH, New York, 2004).
- [14] P. Massignan and G. M. Bruun, *Eur. Phys. J. D* **65**, 83 (2011).
- [15] F. Chevy, *Phys. Rev. A* **74**, 063628 (2006); C. Lobo, A. Recati, S. Giorgini, and S. Stringari, *Phys. Rev. Lett.* **97**, 200403 (2006); N. V. Prokof'ev and B. V. Svistunov, *Phys. Rev. B* **77**, 020408 (2008); G. M. Bruun and P. Massignan, *Phys. Rev. Lett.* **105**, 020403 (2010).
- [16] G. M. Bruun, A. Recati, C. J. Pethick, H. Smith, and S. Stringari, *Phys. Rev. Lett.* **100**, 240406 (2008).
- [17] In the case of atomic gases, we also assume that three-body recombination rates are small and do not affect the lifetime.
- [18] G. F. Giuliani and G. Vignale, *Quantum Theory of the Electron Liquid* (Cambridge University Press, Cambridge, England, 2005).
- [19] C. M. Varma, Z. Nussinov, and W. van Saarloos, *Phys. Rep.* **361**, 267 (2002); note, however, that, unlike in this reference, here in this Letter we assume that perturbation theory is valid and  $Z = 1 + O(a^2)$ .
- [20] G. D. Mahan, *Many Particle Physics* (Kluwer, New York, 2010).
- [21] M. Koschorreck, D. Pertot, E. Vogt, B. Fröhlich, M. Feld, and M. Köhl, *Nature (London)* **485**, 619 (2012).
- [22] J. T. Stewart, J. P. Gaebler, and D. S. Jin, *Nature (London)* **454**, 744 (2008).
- [23] A. Sommer, M. Ku, G. Roati, and M. W. Zwierlein, *Nature (London)* **472**, 201 (2011); A. Sommer, M. Ku, and M. W. Zwierlein, *New J. Phys.* **13**, 055009 (2011).